

Development of Press Forming Technologies for Ultra-High Strength Steel Sheets Utilizing Computer Aided Engineering

SHINMIYA Toyohisa^{*1} URABE Masaki^{*2} FUJII Yusuke^{*3}

Abstract:

Problems in press forming, such as fractures and wrinkles, and poor dimensional accuracy due to springback, are much more serious in ultra high strength steels (UHSS) whose tensile strength is more than 780 MPa than in mild steels. JFE Steel has developed various technologies for defect prediction and new forming method utilizing computer aided engineering (CAE). Three of the developed technologies are presented in this paper. Although stretch flange fractures cannot be predicted with the conventional forming limit diagram, it is possible to predict stretch flange fractures accurately by the developed method using not only the maximum principal strain but also the maximum principal strain gradient in the radial direction. In order to find effective solution against springback, a technology of springback factor analysis was developed, which can spot the area holding stresses which govern the springback. Regarding a new forming technology for UHSS's, preforming is effective to improve formability of UHSS's, and optimization method of the preformed shape was developed. The effects of preforming on fractures and wrinkles were verified in the press trials of a front side member and A-pillar lower.

1. Introduction

Reduction of automobile body weight for reducing CO₂ emissions by improved fuel economy and improvement of collision safety (crashworthiness) for passenger protection are maximum principal issues in the devel-

opment of automobiles. High strength steel sheets are applied to automobile structural parts to address these problems. In recent years, application of ultra-high strength steels (UHSS) of tensile strength (TS) 980 MPa class and higher has expanded, and application to hard-to-form parts with curved whole shapes, represented by the front side member and A-pillar lower, is also increasing.

Because the formability of steel sheets generally decreases as material strength increases¹⁾, fracture and wrinkle become problems in cold press forming of UHSS. In addition, it is also more difficult to secure dimensional accuracy, as springback is more serious in UHSS than in mild steels. Rapid progress has been achieved in the finite element method and other CAE techniques in recent years. These techniques are now utilized in study of countermeasures for these problems, and prediction of fracture, wrinkle and springback, as well as development of new cold press forming technologies, has been studied. Prediction and judgment technologies based on CAE analysis are particularly important when using UHSS, as the problems stretch flange fracture from sheared edges and poor dimensional accuracy due to springback are remarkable. JFE Steel developed a stretch flange fracture judgment technology²⁻⁴⁾ using the strain gradient and a springback factor analysis technology^{2,5,6)} which can identify the areas of press bottom dead point stress that are factors in springback.

Moreover, in forming the above-mentioned front side member and other hard-to-form curved parts, a

[†] Originally published in *JFE GIHO* No. 41 (Feb. 2018), p. 34-40



^{*1} Senior Researcher Manager,
Forming Technology Research Dept.,
Steel Res. Lab.,
JFE Steel



^{*2}Dr. Eng.,
Senior Researcher General Manager,
Forming Technology Research Dept.,
Steel Res. Lab.,
JFE Steel



^{*3} Senior Researcher Deputy Manager,
Forming Technology Research Dept.,
Steel Res. Lab.,
JFE Steel

new press forming method which can prevent fracture and wrinkles is necessary. In the general multi-process press forming process, the product shape is formed in the final process after previous forming a shape near the final product shape. JFE Steel developed a pre-forming technology which makes it possible to design the optimum shape in the preforming process before the final process. This report introduces two new press forming methods utilizing this preforming technology^{7,8)}.

2. Stretch Flange Fracture Judgment Technology

A Forming Limit Diagram (FLD) is generally used in fracture predictions in CAE analysis of press forming of steel sheets. However, judgment by this FLD is not possible in the case of fractures that occur at shared edges such as blank edges because the mechanism that leads to fracture is different from the deformation limit given by the FLD. Together with material properties⁹⁾ and shearing conditions^{10,11)}, the stretch flange deformation limit is also influenced by the strain gradient¹²⁾. Although the influence of material properties and shearing conditions has been studied quantitatively, virtually no quantitative study has been devoted to the strain gradient. Therefore, several types of hole expansion tests with different strain gradients were conducted using various types of steel sheets in order to clarify the influence of the strain gradient on the stretch flange deformation limit quantitatively, and a method for prediction of stretch flange fracture by CAE analysis was developed.

2.1 Influence of Strain Gradient on Stretch Flange Limit

The stretch flange deformation limit is strongly influenced by the gradient of the maximum principal strain in the perpendicular direction (radial direction) to the maximum principal strain of the sheared edge (circumferential direction). In the following, this gradient is called the radial strain gradient. This section presents the results of an investigation of the influence of the radial strain gradient on the critical maximum principal strain for fracture (critical strain for fracture).

2.1.1 Experimental conditions

As test materials, the five types of steel sheets from mild steel to 980 MPa class high strength steel (sheet thickness: 1.2 mm) shown in **Table 1** were prepared, and various types of hole expansion tests were conducted. The experimental conditions of the hole expansion tests are shown in **Table 2**. Using three levels of initial punched hole diameters and two types of punch shapes (60° conical shape and flat-bottomed

Table 1 Mechanical properties of examined steels

Steel	YS (MPa)	TS (MPa)	EI (%)	λ (%)
A	168	309	49	155
B	330	459	35	107
C	419	643	28	62
D	603	823	20	71
E	787	1 005	18	47

λ : Hole expansion ratio with conical punch

Table 2 Experimental conditions of hole expansion tests

initial hole diameter in blank (mm)	Punch shape	Applied steel
10, 25, 50	60°conical	A, B, C, D, E
10	ϕ 50 mm cylindrical	A, B, C
25	ϕ 80 mm cylindrical	A, B, C
	ϕ 50 mm cylindrical	D, E
50	ϕ 150 mm cylindrical	A, B, C
	ϕ 100 mm cylindrical	D, E

cylindrical shape), hole expansion tests were carried out under a total of six conditions, representing the various combinations of these hole diameters and punch shapes. The punch clearance relative to the sheet thickness was constant at 12.5%, and in the tests with the cylindrical punches, the punch diameter was changed as necessary corresponding to the material properties so that the fracture position was the hole edge.

2.1.2 Influence of radial strain gradient on critical strain for fracture

The influence of the radial strain gradient on the critical strain for fracture at the hole edge is shown in **Fig. 1**. Assuming that the strain of the hole edge is uniform in the circumferential direction, the critical strain

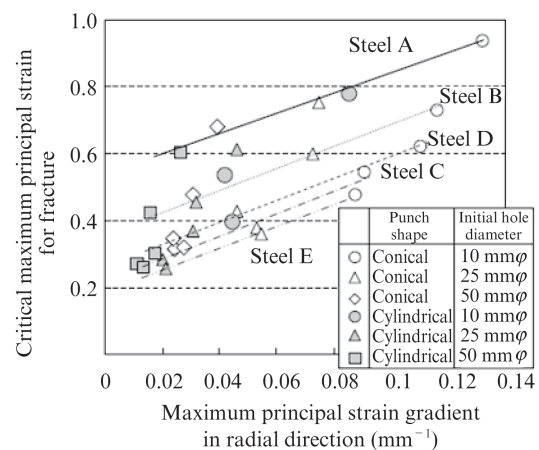


Fig. 1 Effect of maximum principal strain gradient in radial direction on critical strain for fracture

for fracture was calculated from the limit hole expansion ratio. The radial strain gradient was defined as the average gradient of the maximum principal strain in a radial distance of 5 mm from the hole edge at the fracture hole diameter and was calculated by CAE. The software used in the CAE was LS-DYNA™ ver.971 (Livermore Software Technology Corp.). As a result, the critical strain at the hole edge was different depending on the material, but with all of the materials, it was found that the critical strain increased a substantially linear manner as the radial strain gradient increased. This behavior is thought to be due to an increase in the strain localization suppression effect due to the fact that the interior of the material does not achieve a strain localization condition of uniaxial tension, even when such a condition is achieved at the hole edge, and an increase in the necking growth suppression effect^{12,13)} of the region where strain is small.

From the study outlined above, it can be understood that the fracture limits of all the test materials can be arranged by the radial strain gradient and the maximum principal strain at the hole edge, irrespective of forming conditions such as the initial punched hole diameter and shape of the hole expansion punch.

2.1.3 Influence of clearance on critical strain

The hole expansion ratio of high strength steel sheets changes greatly depending on the clearance during shearing¹⁰⁾; hence, in addition to the radial strain gradient, the clearance should also be considered when judging the possibility of forming stretch flange deformation parts. Therefore, the critical strain considering the clearance was studied using steel B as the test material.

Using a blanking clearance condition of approximately 30%, at which the critical strain is assumed to be the smallest¹⁰⁾, a conical hole expansion test with a punched diameter of 10 mm and a tensile test with a strip-type specimen were performed to investigate the influence of the blanking clearance on the critical strain.

Figure 2 shows the result when the limit line for the blanking clearance of approximately 30% was added to the results for steel B in Fig. 1. From Fig. 2, it can be understood that the critical strain is strongly influenced by the blanking clearance in addition to the radial strain gradient. Thus, if the possibility of forming the stretch flange deformation part in a CAE analysis is judged by the limit line considering the blanking clearance and the strain gradient, forming is possible in Zone 1 and impossible in Zone 3. In Zone 2, it is important to control the clearance so that forming is possible, that is, fracture is avoided, according to the clearance during edge shearing.

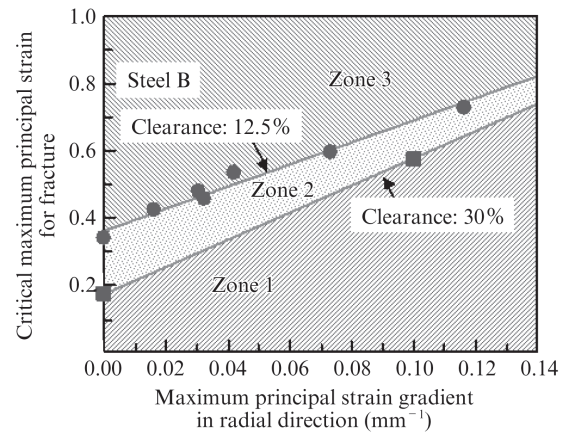


Fig. 2 Effect of maximum principal strain gradient in radial direction on critical strain for fracture considering blanking clearances

2.2 Application to CAE Forming Analysis

From the results up to the previous section, it can be understood that prediction of stretch flange fracture is possible by using the radial strain gradient and the critical strain of the material. This section describes the results of a judgment performed with an actual part shape when this judgment method was incorporated in a general CAE analysis.

2.2.1 Results of actual press forming

A press experiment was performed with a trial die of a B-pillar lower using two types of 590 MP class galvanized steel sheets (hereinafter, GA; thickness: 1.2 mm) with different hole expansion properties (λ). The overall shape of the pressed part is shown in **Photo 1**, and the mechanical properties of the materials are shown in **Table 3**. JEFORMA™ 590 GA Type 2,



Photo 1 Whole appearance of pressed part of B pillar model

Table 3 Mechanical properties of steel used in press forming

Steel	YS (MPa)	TS (MPa)	EI (%)	λ (%)
JEFORMA™ 590GA Type2	437	624	34	92
Conventional 590DP-GA	398	640	32	68

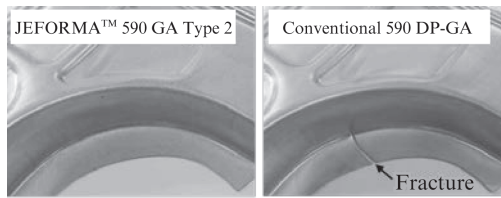


Photo 2 Result of press forming experiment

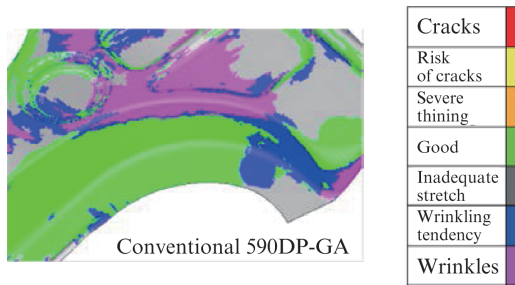


Fig. 3 Fracture judgment using conventional FLD

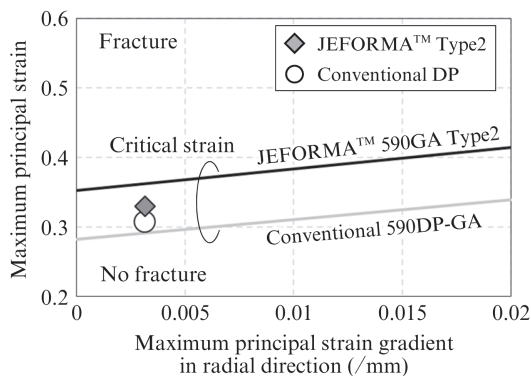


Fig. 4 Fracture evaluation using strain gradient in radial direction

which is one of JFE Steel's high formability high strength steel sheets, is a high EI-high λ type material, and its hole expansion ratio is more than 20% higher than that of the conventional DP material. With the conventional DP material, fracture occurred in the stretch flange deformation part, as shown in **Photo 2**.

2.2.2 Results of press forming analysis

A CAE analysis was performed under the same condition of the test of the fractured conventional DP material. **Figure 3** shows the result of an evaluation using an FLD, which is generally used in fracture judgments. As the judgment result was no fracture, it can be understood that an accurate judgment of stretch flange fracture is not possible with the conventional FLD.

Figure 4 shows the result when the results of a CAE prediction of the strain gradient in the direction perpendicular to the strain at the flange edge (maximum

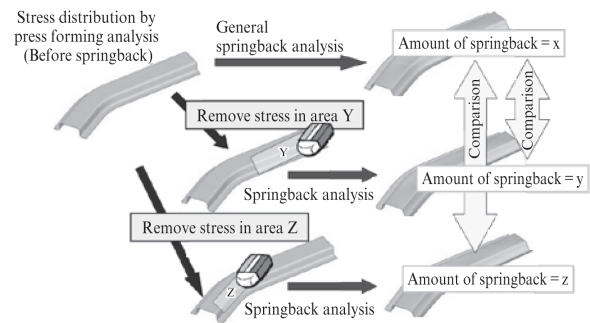


Fig. 5 Schematic diagram of springback factor analysis

principal strain) in the area where the fracture occurred in the press forming experiment were plotted together with the stretch flange limit line. In these results, the conventional DP material is located on the upper side of the fracture limit line, and it was judged that fracture occurs. These CAE results are in agreement with the fracture condition in the experimental results, demonstrating that the stretch flange fracture evaluation technique using the strain gradient is also valid for actual parts.

3. Springback Factor Analysis Technology

Because the springback that occurs when press forming UHSS is extremely large, many die corrections are necessary in order to obtain the target accuracy by the conventional springback-estimated-die technique. To reduce springback, it is necessary to designate the stresses that cause springback and take measures to reduce those stresses. In order to implement effective measures in automotive parts with complex shapes, JFE Steel developed a springback factor analysis technique which designates the factor stresses by CAE analysis.

3.1 Procedure of Springback Factor Analysis

Springback is a type of deformation that occurs when the stress (bottom dead point stress) which exists in a formed part at the bottom dead point in press forming is released accompanying die release. The developed springback factor analysis technique establishes the relationship between springback behavior and bottom dead point stress. In this method, the result of a springback analysis in which the bottom dead point stress in a certain designated region is replaced with zero, and the result of a springback analysis by the conventional method as a standard, are compared so as to identify the influence of the bottom dead point stress in the above-mentioned designated region on springback. A schematic diagram of the springback factor analysis technique is shown in **Fig. 5**.



Fig. 6 Part shape of front pillar reinforcement

Table 4 Mechanical properties of steel used

Steel	YS (MPa)	TS (MPa)	EI (%)	r-value
JAC980Y	687	1 011	19	0.9

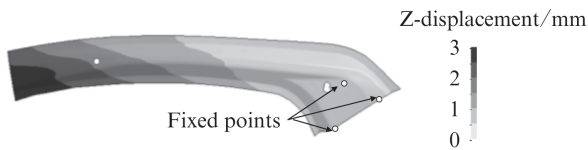


Fig. 7 Springback analysis result

3.2 Springback Factor Analysis Using Actual Part

3.2.1 Object part and test material

The springback factor analysis technique described above was applied to a part simulating a front pillar reinforcement, which is an automobile structural part. The part shape is shown in **Fig. 6**. Because this part is long and thin and is curved in the longitudinal direction, complex springback such as torsion, camber, etc. occur. Press forming was performed by a single-process bending without using a pad. The test material was a 980 MPa class GA steel sheet with a sheet thickness of 1.4 mm. The mechanical properties of the steel are shown in **Table 4**.

3.2.2 Result of springback factor analysis

LS-DYNA™ ver.971 was used in the press forming analysis and springback analysis necessary in the springback factor analysis.

As a result of the springback analysis, torsion and camber occurred in the longitudinal direction, as shown in **Fig. 7**. In this report, a factor analysis of torsion was performed. Torsion was evaluated by setting three fixed points on the right side of the part, as shown in **Fig. 7** and evaluating torsion from the twist angle calculated from two points at the end of the left side of the part. The twist angle of the part by this evaluation method was 3.9°.

The bottom dead point stress in press forming includes a complex distribution of tensile and compressive stresses over the entire part, as shown in **Fig. 8**.

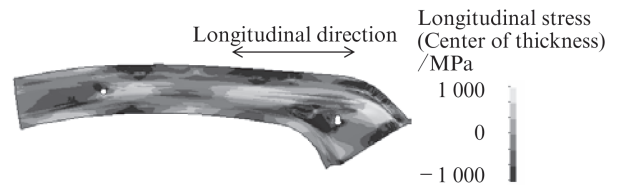


Fig. 8 Stress distribution at bottom dead point before springback

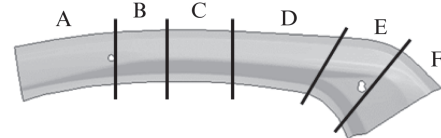


Fig. 9 Divided 6 areas for springback root cause analysis

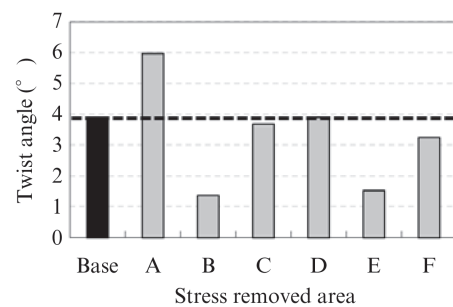


Fig. 10 Effect of stress at bottom dead point in each areas on twist angle

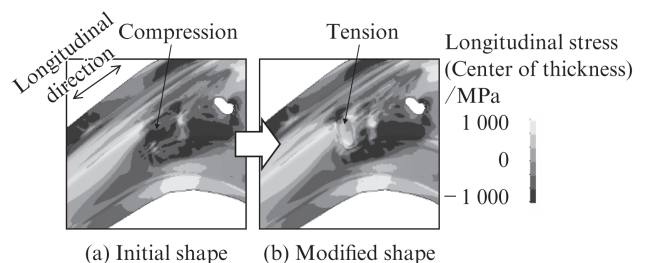


Fig. 11 Added bead shape and change in stress distribution at bottom dead point in press forming

The evaluation in the springback factor analysis was performed by dividing the part into the six regions from A to F, as shown in **Fig. 9**. The evaluation results are shown in **Fig. 10**. It can be understood that the stresses in regions B and E have actions that reduce the twist angle. Accordingly, it is estimated that the twist angle can be decreased by reducing the stresses in region B and E by applying ingenuity to the forming method and part shape.

Therefore, a springback countermeasure for the compressive stress in region E was studied. As a result of the investigation of factors that cause compressive stress, it is thought that excess material is generated during the forming process, and compressive stress is

generated at the bottom dead point due to forming of that excess material. Accordingly, as a countermeasure, a concave part was added in the area of compressive stress. **Figure 11** shows the added concave shape (bead) and the stress distribution at the bottom dead point. It was found that addition of the concave part changed the compressive stress that existed in region E to tensile stress, and the result of the springback analysis confirmed that the twist angle was reduced substantially, from 3.9° to 2.2°.

4. Development of New Press Forming Method by Applying Preforming Technology

In conventional multi-process press forming, the blank is formed to near the final part shape in the previous process, and is then formed to the final shape in the following restrike process. Since UHSS are characterized by low ductility and high yield strength, the problems of fracture and wrinkle become apparent in hard-to-form parts with curved whole shapes, such as the front side member and the A-pillar lower. A preforming technology which effectively uses each of these multiple processes was developed to solve these problems. As the preformed part shape in the preceding process is critical when using this technology, a design method and preforming method for the optimum shape were developed by utilizing CAE.

4.1 Application to Front Side Member Model

When forming parts having a curved shape as seen from the side, represented by the front side member, by the conventional drawing process, excess/insufficient material is generated on the inner and outer sides of the curve. Therefore, as shown in **Photo 3**, fracture on the outer side of the curve and wrinkles on the inner side are problems. Because application of in-plane shearing deformation to the longitudinal wall, as illustrated in **Fig. 12**, is effective for suppressing these problems, a preforming method which makes it possible to introduce in-plane shear deformation in the region corresponding to the longitudinal wall was developed. The preforming process is deep drawing forming of a strip-type blank, as shown in **Photo 4(a)**, and makes it possible to apply in-plane shearing deformation to the region corresponding to the longitudinal wall. The part

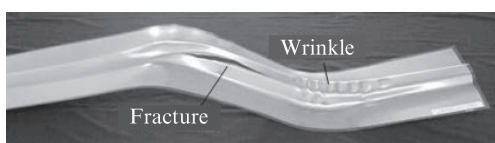


Photo 3 Front side member formed by conventional draw process

can then be formed to the final part shape by bending the ridge line in the following process. The results of trial production by the developed method using a 1 180 MPa class GA steel sheet (thickness: 1.6 mm) having the mechanical properties shown in **Table 5** confirmed that it is possible to prevent fracture and wrinkle, as shown in Photo 4(b).

4.2 Application to A-Pillar Lower Model

Viewed from above, the A-pillar lower is a curved L-shaped structural part. In the conventional drawing process, as shown in in **Fig. 13**, wrinkle, which occurs in the top plate of the curved part, and fracture during drawing-stretch forming, which occurs at the punch shoulder in the lower part of the vehicle, are problems.

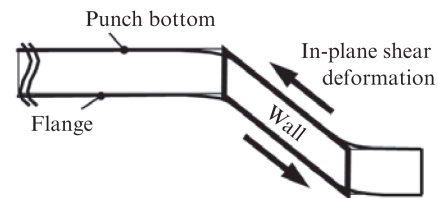


Fig. 12 In-plane shear deformation in wall area

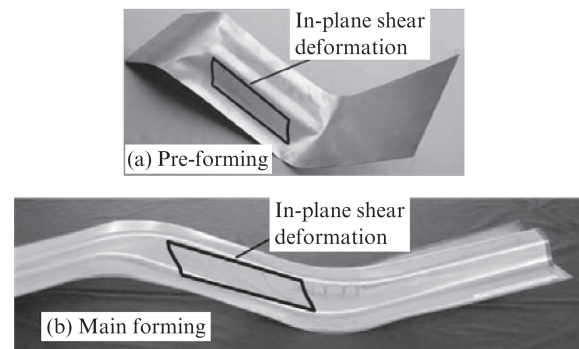


Photo 4 Trial parts: (a) pre-forming, (b) main forming

Table 5 Mechanical properties of steel used

Steel	YS (MPa)	TS (MPa)	EI (%)
JAC1180YL	819	1 234	11

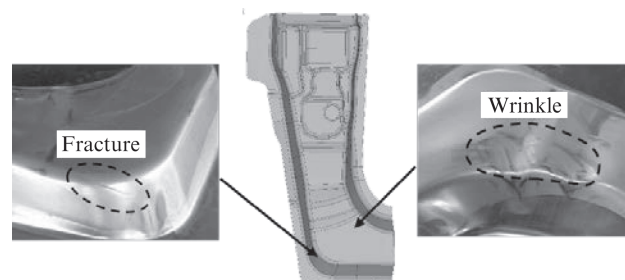


Fig. 13 Part shape of A pillar lower and problems in press forming

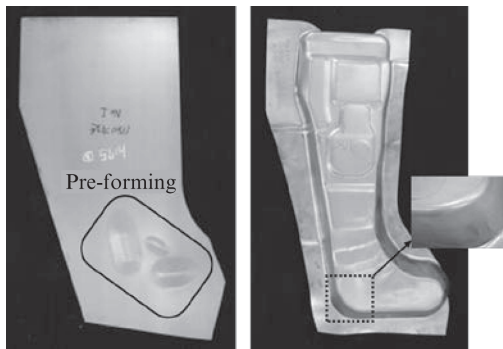


Fig. 14 Localized pre-formed blank and pressed part

Table 6 Mechanical properties of steel used

Steel	YS (MPa)	TS (MPa)	EI (%)
JAC1180YL	878	1 182	10

Since it is possible to prevent wrinkle by applying a localized pad to the part where wrinkle occurs, application of preforming was studied as a countermeasure for fracture.

Fracture in the lower part of the vehicle occurs because the supply of material to the punch shoulder from the surrounding area is insufficient and strain concentrates locally. Therefore, a locally stretched pre-formed shape was applied at the appropriate position in the blank with the aim of dispersing the strain by supplying material to the part with a danger of fracture at the punch shoulder from the low strain region at the punch bottom (top plate) during forming. **Figure 14** shows the blank that was given the optimum localized stretch preforming and the trial product that was formed by drawing with a localized pad when using that blank. The material used in the trial production was a 1 180 MPa class GA steel sheet (thickness: 1.4 mm) with the mechanical properties shown in **Table 6**. It was shown that fracture and wrinkle can be prevented by localized stretch preforming and use of the localized pad. Moreover, it is also possible to reduce the number of manufacturing processes and die costs by forming preformed shapes in the blanking process.

5. Conclusion

Because cold press forming of UHSS will also be applied widely to automobile structural parts in the future, countermeasure technologies for the problems of fracture, wrinkle and poor dimensional accuracy were developed.

Although stretch flange fracture cannot be judged by the conventional FLD, a technology for prediction of stretch flange fracture using the strain gradient was developed, and as a result, accurate prediction is now possible.

Development of a springback factor analysis technology for designating parts that cause poor dimensional accuracy and areas of stress made it possible to propose effective springback countermeasures.

As a new press forming method for hard-to-form parts with curved shapes, such as the front side member and the A-pillar lower, a method applying a preforming technology for design of the optimum preformed part shape before the final forming process was developed, and its effectiveness in preventing fracture and wrinkle was confirmed by trial production of model parts using the developed method.

References

- 1) Urabe, T.; Hosoya, Y. *Journal of the Japan Society for Technology of Plasticity*. 2005, vol. 46, no. 534, p. 560–564.
- 2) Ishiwatari, A.; Urabe, M.; Inazumi, T. *JFE Technical Report*. 2013, no. 18, p. 96–102.
- 3) Iizuka, E.; Urabe, M.; Yamasaki, Y.; Inazumi, T. *Journal of the Japan Society for Technology of Plasticity*. 2010, vol. 51, no. 594, p. 700–705.
- 4) JFE Steel. Iizuka, Eiji. Japanese Patent 4935713.
- 5) Hiramoto, J.; Urabe, M.; Ishiwatari, A.; Urabe, T.; Yoshida, F. *Journal of the Japan Society for Technology of Plasticity*. 2015, vol. 56, no. 658, p. 955–960.
- 6) JFE Steel. Urabe, Masaki. Japanese Patent 4894294.
- 7) JFE Steel. Fujii, Yusuke. Japanese Patent 6112226.
- 8) JFE Steel. Shinmiya, Toyohisa. Japanese Patent 6191846.
- 9) Nakagawa, T.; Takita, M.; Yoshida, K. *Journal of the Japan Society for Technology of Plasticity*. 1970, vol. 11, no. 109, p. 142–151.
- 10) Iizuka, E.; Hira, T.; Yoshitake, A. *Journal of the Japan Society for Technology of Plasticity*. 2005, vol. 46, no. 534, p. 625–629.
- 11) Toyoda, D.; Sato, Y.; Urabe, M.; Tamai, Y.; Yoshitake, A. *The 58th Proceedings of the Japanese Spring Conference for the Technology of Plasticity*. 2007, p. 537–538.
- 12) Nakagawa, T. *Journal of the Japan Society for Technology of Plasticity*. 1978, vol. 19, no. 206, p. 227–235.
- 13) Goto, M. *Journal of the Japan Society for Technology of Plasticity*. 1993, vol. 34, no. 388, p. 454–461.